Design, Considerations, and Implementation of a Solar-Powered Smart Street Lighting System with Integrated CCTV and IoT-Based Monitoring

Muhammad Rizani Rusli[*,a,1], Rachma Prilian Eviningsih[a,2], Lucky Pradigta Setiya Raharja[a,3], Luki Septya Mahendra[a,4], Achmat Ridwan Nudin[a,5], Naufal Fadhlirahman Dheningrat[a,6], Akmal Fikri[a,7], Mentari Putri Jati[b,8]
[a]Politeknik Elektronika Negeri Surabaya, Surabaya, Indonesia
[b]Research Center for Information Technology, Academia Sinica, Taipei, Taiwan

*Corresponding Author: rizani@pens.ac.id

Abstract

This study presents the design, implementation, and short-term experimental validation of a standalone solar-powered smart street lighting system integrating LED illumination, CCTV surveillance, and Internet of Things (IoT)-based real-time monitoring within a single pole-mounted platform. Load profiling identified a total energy demand of 1176 Wh/day, which increased to 1529 Wh/day after applying a 30% design margin. These requirements guided the selection of a 460 Wp monocrystalline photovoltaic module, a 40 A maximum power point tracking charge controller, and a 12.8 V, 150 Ah $LiFePO_4$ battery. Laboratory testing demonstrated the expected bulk/MPPT, boost, and float charging stages, while accelerated battery testing at 0.27C measured a capacity of 151 Ah. During five consecutive days of field testing under sunny to partly cloudy conditions, the post-charging state of charge (SOC) ranged from 90.0% to 97.2%, while the next-morning SOC ranged from 58.6% to 68.4%. The average nighttime SOC reduction was 32.8%, with a range of 25.1% to 37.3%. The IoT platform provided real-time monitoring of photovoltaic generation, battery condition, and load operation, while maintaining communication availability above 99% during the observation period. These results demonstrate short-term autonomous operation and technical feasibility under the observed field conditions. Longer seasonal testing and a complete life-cycle economic assessment remain necessary to evaluate long-term reliability and financial feasibility.

Keywords: Solar Street Lighting, Standalone Photovoltaic System, MPPT Solar Charge Controller, $LiFePO_4$ Battery, IoT-Based Monitoring.

I. Introduction

Rapid urbanization and the increasing complexity of metropolitan environments have accelerated the adoption of smart city concepts to address challenges related to energy sustainability, public safety, and infrastructure efficiency. Smart cities leverage information and communication technologies (ICT), renewable energy resources, and Internet of Things (IoT) platforms to enhance operational performance and improve urban services. Within this context, public street lighting represents a fundamental urban infrastructure, providing not only nighttime illumination but also improved traffic safety and urban security. However, conventional grid-powered lighting systems remain energy-intensive, costly to operate, and vulnerable to outages, particularly in rapidly growing cities and developing regions [1], [2].

From an energy perspective, street lighting contributes significantly to municipal electricity expenditure, accounting for approximately 1–1.5% of national electricity consumption and up to 30–50% of local government energy costs in some cities [2]. Traditional technologies such as high-pressure sodium and mercury vapor lamps suffer from low luminous efficacy, limited lifetimes, and high maintenance requirements. In contrast, light-emitting diode (LED) luminaires offer energy savings of 50–80%, luminous efficacy above 150 lm/W, and lifetimes exceeding 50,000–100,000 hours, resulting in lower operational and maintenance costs [2], [3], [4], [5]. These advantages have promoted the transition toward LED-based smart lighting systems integrated with digital control and monitoring platforms.

The integration of renewable energy further enhances the sustainability of lighting infrastructure. Solar photovoltaic (PV) technology has experienced rapid global growth and now represents one of the largest contributors to renewable electricity generation, accounting for approximately 4.5% of global output [6]. Continuous improvements in conversion efficiency and declining system costs strengthen the feasibility of PV-powered applications [7], [8], [9]. Nevertheless, PV performance is strongly affected by irradiance variability, temperature, and environmental factors, necessitating maximum power point tracking (MPPT) techniques to optimize energy harvesting, which can improve efficiency by up to 30–40% compared to fixed operating points [10], [11], [12], [13].

Indonesia, located near the equator, possesses abundant solar potential suitable for off-grid public infrastructure. Surabaya, one of the largest metropolitan cities in the country, has actively implemented smart city initiatives and achieved high rankings in the Indonesia Smart City Index through ICT integration and sustainable development programs [14], [15]. Deploying solar-powered lighting systems aligns with these initiatives by reducing dependence on fossil-fuel-based electricity, lowering operational costs, and improving resilience during grid disturbances [10], [16]. In addition, urban safety remains a priority, particularly in areas with higher crime rates, where continuous surveillance is required. Integrating CCTV and communication devices into lighting poles provides efficient infrastructure utilization but introduces continuous 24-hour loads that demand reliable energy storage and system-level management [17].

Previous studies have investigated solar-powered street lighting, adaptive illumination, IoT-based monitoring, and smart utility poles [18], [19], [20], [21], [22], [23]. However, the literature reviewed in this study primarily addresses these functions separately or evaluates prototype-scale lighting control systems [3], [24]. Limited experimental evidence is available for a full-scale pole-mounted system that simultaneously integrates photovoltaic generation, $LiFePO_4$ storage with battery management, CCTV surveillance, coordinated AC and DC protection, and real-time monitoring of generation, storage, and load parameters. Furthermore, few studies report both controlled laboratory characterization and field-scale energy-balance evaluation within the same implementation framework.

To address this gap, this study designs, implements, and evaluates a standalone solar-powered smart street lighting pole integrating LED illumination, CCTV surveillance, and IoT-based monitoring. The main contributions are: (i) systematic load, photovoltaic, battery, and electrical-protection sizing for a multifunctional smart pole; (ii) hardware integration of photovoltaic generation, $LiFePO_4$ storage, AC and DC loads, surveillance, and remote monitoring within a single pole-mounted platform; and (iii) laboratory characterization of battery and MPPT operation followed by five-day field validation of SOC variation, energy consumption, and communication availability. The study focuses on short-term technical feasibility, while seasonal reliability and complete life-cycle economics are identified as subjects for further investigation.

II. METHOD

This study adopts an engineering design–implementation methodology to develop and validate a standalone solar-powered smart street lighting pole that integrates LED illumination, CCTV surveillance, and IoT-based real-time monitoring within a single autonomous infrastructure. The methodological framework combines analytical load assessment, photovoltaic (PV) and battery sizing, component selection, electrical protection coordination, and system-level hardware–software integration to ensure reliable off-grid operation under realistic urban environmental conditions. The overall workflow begins with quantification of the electrical demand profile, which serves as the basis for determining energy generation and storage requirements. Subsequently, appropriate power conditioning devices, protection schemes, and monitoring subsystems are incorporated to achieve operational safety, efficiency, and maintainability. All subsystems are then physically integrated into a compact pole-mounted configuration to enable practical field deployment.

A. Load Profile and Energy Demand Analysis

Accurate load estimation constitutes the foundation of standalone PV system design because generation capacity, storage requirements, and economic feasibility are directly dependent on daily energy demand. In off-grid applications, miscalculation may propagate throughout the design process, leading either to undersized systems that compromise reliability or oversized installations that increase capital costs unnecessarily [26], [27]. Therefore, a detailed load profiling procedure is conducted to evaluate the operational requirements of each subsystem.

The proposed smart pole comprises three primary loads: (i) a 30 W LED luminaire operating for 12 h during nighttime, (ii) a CCTV camera operating continuously for 24 h, and (iii) an IoT communication modem operating continuously. The instantaneous electrical power of each load is defined by (1).

$$P_i = V_i \; x \; I_i \tag{1}$$

The daily energy consumption of each load is calculated as (2). Where E_i represents the daily energy consumption (Wh/day) and t_i is the daily operating duration (h/day).

$$E_i = P_i \; x \; t_i \tag{2}$$

The total daily electrical energy demand of the system is obtained by summing the energy consumption of all individual loads as in (3). To account for system losses and non-ideal operating conditions, the design energy requirement is defined by applying a safety factor k as in (4). Where k>1 represents the loss compensation factor. In this study, a value of $k = 1.3$ is adopted to accommodate conversion losses, wiring losses, temperature effects, and inverter inefficiencies.

$$E_{total} = \sum_{i=1}^{n} E_i \tag{3}$$

$$E_{design} = \; k \; x \; E_{total} \tag{4}$$

Using this formulation, the lighting load consumes 360 Wh/day, the CCTV consumes 576 Wh/day, and the modem consumes 240 Wh/day, yielding E_{total}=1176 Wh/day. After applying the safety margin, the design energy requirement becomes E_{design}=1529 Wh/day. The rated power of each device was used as a conservative design input to prevent undersizing of the photovoltaic and battery subsystems.

LED technology is selected due to its high luminous efficacy (>150 lm/W), long lifetime (>50,000 h), and compatibility with intelligent control systems, making it well suited for solar-powered and smart city applications [2]. Although LED luminaires may be directly supplied by DC sources, an AC-based commercial luminaire is adopted for standardization and maintenance practicality; hence, a pure sine-wave inverter is employed to minimize harmonic distortion and extend driver lifetime [28], [29].

B. Photovoltaic Calculation and Consideration

Photovoltaic systems convert solar energy into electrical energy through the photovoltaic effect [8]. The photovoltaic subsystem is sized to satisfy the design energy requirement while maintaining operational reliability under varying irradiance. Among available PV technologies, monocrystalline silicon modules are selected due to their superior conversion efficiency, compact form factor, and suitability for pole-mounted installations with limited surface area [7], [30].

The required PV capacity is estimated using the Peak Sun Hour (PSH) method [30]. Assuming a conservative PSH of 4.5 h for Surabaya, the minimum capacity is calculated by (5).

$$P_{pv} = \frac{E_{design}}{PSH} = \frac{1529}{4.5} = 339.77 \; Wp \tag{5}$$

To improve operational reliability and provide sufficient margin under cloudy or partially shaded conditions, a single 460 Wp monocrystalline PV module is selected. The expected daily energy production from the selected module, E_{pv} in Wh/day is calculated as in (6).

$$E_{pv} = 460 \; x \; 4.5 = 2070 \; Wh/day \tag{6}$$

$$E_{usable} = 0.9 \; x \; 2070 = 1863 \; Wh/day \tag{7}$$

Assuming an overall system efficiency of 90%, which accounts for MPPT conversion losses, wiring losses, and temperature derating, the usable daily energy, E_{usable} becomes (7). This value exceeds the required daily energy consumption, ensuring adequate energy reserve for stable battery charging and continuous system operation. A single-module configuration is intentionally adopted to simplify wiring, minimize mismatch losses, reduce installation complexity, and enhance reliability. Multi-module arrays are susceptible to current–voltage mismatches that may reduce output power by up to 25% [31], [32].

C. Solar Charge Controller System

The PV output must be regulated before battery storage to prevent overcharging and premature degradation. Therefore, a Maximum Power Point Tracking (MPPT) solar charge controller is employed. MPPT controllers dynamically adjust operating voltage to extract maximum available power under varying irradiance and temperature conditions, offering higher energy utilization compared with PWM-based alternatives [13], [33], [34], [35].

Given the 460 Wp module and 12 V battery system, the maximum theoretical charging current can be approximated as in (8).

$$I_{chargemax} = \frac{P_{pv}}{V_{batt}} = \frac{460}{12} = 38.3\ A \quad (8)$$

Accordingly, a 40 A MPPT controller is selected to provide safe thermal margins and long-term reliability. The controller also integrates protection against overcharge, overdischarge, overload, and overheating, thereby ensuring autonomous field operation.

D. Battery Energy Storage System and Battery Management

Proper battery sizing is essential to ensure system reliability, extend service life, and prevent premature degradation, since the selected capacity directly influences operational constraints and long-term performance [36]. The Battery Energy Storage System (BESS) guarantees continuous power supply during nighttime and low-irradiance periods.

Lithium iron phosphate ($LiFePO_4$) chemistry is selected due to its high cycle life, superior thermal stability, deep discharge capability, and intrinsic safety compared with conventional lead-acid batteries [37]. A blade-type prismatic cell configuration is adopted to enhance mechanical strength, improve volumetric compactness, and facilitate integration within the street lighting pole structure [38].

Considering the mechanical constraints of pole-mounted solar street lighting, the elongated blade geometry enables a linear and slim arrangement compatible with the cylindrical lighting pole. Consequently, the battery pack is arranged longitudinally and mounted vertically within the pole structure below the PV module to optimize space utilization and simplify installation. The enclosure is constructed from galvanized metal for corrosion resistance, while all external connectors are rated IP66. The assembly is fully sealed to provide waterproof and dustproof protection suitable for outdoor environments. The mechanical configuration of the battery pack is illustrated in Figure 1.

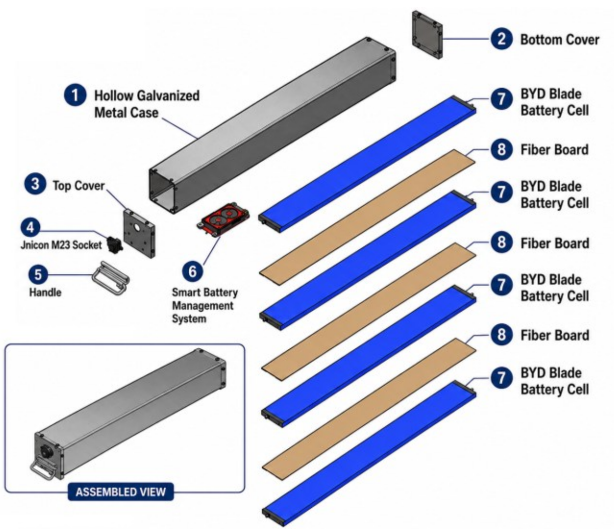

Figure 1. Proposed Battery Energy Storage System

Battery capacity is determined from the daily energy demand, system voltage, allowable DoD, and required autonomy. For the proposed system, E_{total} denotes the daily load energy (Wh/day), E_{total} = 1176 Wh/ day, while N_{aut} represents the autonomy duration (days), $N_{aut} = 1$ day. The required battery energy capacity is defined as (9). Considering DoD limitations at 0.8, the nominal rated energy becomes (10). The corresponding battery capacity in ampere-hours, C_{Ah} is calculated as (11) with the battery system voltage, V_{sys}=12.8V.

$$E_{bat} = E_{total}\ x\ N_{aut} = 1176\ x\ 1 = 1176\ Wh \tag{9}$$

$$E_{rated} = \frac{E_{bat}}{DoD} = \frac{1176}{0.8} = 1470\ Wh \tag{10}$$

$$C_{Ah} = \frac{E_{rated}}{V_{sys}} = \frac{1470}{12.8} = 114.8\ Ah \tag{11}$$

Thus, the minimum required capacity is 114.8 Ah. To provide a safety margin for aging, temperature variations, and conversion losses, a 150 Ah battery is selected (C_{Ah_select}). The usable energy capacity can be calculated using (12), and the resulting autonomy (N_{aut_actual}) is obtained in (13). Hence, the selected $LiFePO_4$ battery provides sufficient usable energy and extended autonomy to maintain reliable operation during low-solar or cloudy conditions.

$$E_{usable,batt} = V_{sys}\ x\ C_{Ah\_select}\ x\ DoD = 12.8\ x\ 150\ x\ 0.8 = 1536\ Wh \tag{12}$$

$$N_{aut\_actual} = \frac{E_{usable}}{E_{total}} = \frac{1536}{1176} = 1.3\ days \tag{13}$$

E. Electrical Protection System Design

The proposed standalone photovoltaic (PV) street lighting system integrates a 460 Wp PV generator, an MPPT charge controller, a 12.8 V lithium battery energy storage system (BESS), low-voltage DC loads, and a single-phase AC inverter. Since the system operates on a low-voltage, high-current DC architecture, the dominant electrical risks include short-circuit currents, overload conditions, surge transients, and battery-related faults. Therefore, a coordinated multi-layer protection strategy is implemented to ensure operational safety, equipment reliability, and selective fault isolation. The protection framework combines surge protection devices (SPD), fuses, DC miniature circuit breakers (MCB), a smart Battery Management System (BMS), and an AC residual current breaker with overcurrent protection (RCBO).

At the PV input stage, protection is designed according to standard PV safety multipliers. With a typical maximum power voltage of approximately 41 V, the operating current is calculated in (14). Considering the short-circuit margin as in (15). Following standard PV protection practice, the fuse rating is selected as in (16). Therefore, the PV-side protection is specified as a 25 A DC fuse and a 25 A DC MCB.

$$I_{maximumpower} = \frac{P_{pv\_actual}}{V_{maximumpower}} = \frac{460}{41.55} = 11.07\ A \tag{14}$$

$$I_{sc} = 1.25\ x\ I_{maximumpower} = 1.25\ x\ 11.07 = 13.83\ A \tag{15}$$

$$I_{fuse} \geq 1.56\ x\ I_{sc} = 21.57\ A \tag{16}$$

The battery subsystem consists of a 12.8 V, 150 Ah $LiFePO_4$ pack equipped with a 100 A smart BMS providing cell-level monitoring and electronic protection. The battery branch current was evaluated separately for charging and discharging conditions because the MPPT charging current and load-discharge current flow in opposite directions. During charging, the maximum controller output current is 40 A. During discharging, the maximum estimated current is approximately 25 A, comprising the inverter and auxiliary DC loads. Therefore, the maximum battery-branch operating current is determined as in (17).

$$I_{protect\_batt} = \max(I_{charge}, I_{discharge}) = \max(40, 25) = 40\ A \tag{17}$$

A 63 A DC MCB was selected to accommodate the maximum branch current and transient conditions while remaining below the 100 A BMS protection threshold. The MCB rating was also coordinated with the current-carrying capacity of the battery conductors.

For the low-voltage DC branch, the modem (10 W) and CCTV unit (24 W) produce a combined demand of 34 W. Applying a 125% design factor, the protection current is calculated using (18). A 6 A DC MCB is therefore selected to accommodate transient startup currents from DC–DC converters while ensuring adequate overload and short-circuit protection.

$$I_{protect\_DCload} = 1.25\ x\ \frac{P_{DCload}}{V_{sys}} = 1.25\ x\ \frac{34}{12.8} = 3.4\ A \tag{18}$$

The inverter supplies a 30 W LED lamp and a 100 W AC outlet, resulting in a total AC load of 130 W. Considering an inverter efficiency of 85%, the required DC input power becomes (19) including a 125% design margin. A 20 A DC MCB is therefore adopted to accommodate continuous operation and inverter inrush currents while ensuring reliable short-circuit protection.

$$I_{protect\_inverter} = 1.25\ x\ \frac{\frac{P_{ACload}}{0.85}}{V_{sys}} = 1.25\ x\ \frac{\frac{130}{0.85}}{12.8} = 14.935\ A \tag{19}$$

On the AC side, the maximum current is calculated using (20). A 3 A residual current circuit breaker with overcurrent protection (RCBO) is installed to provide both overload protection and earth-leakage detection. This device enhances user safety by preventing electric shock hazards and insulation faults at the load terminals.

$$I_{protect\_AC} = 1.25\ x\ \frac{P_{ACload}}{220} = 1.25\ x\ \frac{130}{220} = 0.74\ A \tag{20}$$

Selective coordination ensures localized fault isolation without interrupting the entire system, improving reliability and maintainability. A summary of protection ratings is presented in Table 1.

Table 1. Summary of Protection Ratings

Location	Device Type	Rating
PV string	Fuse + DC MCB	25 A
Battery main	DC MCB	63 A
DC load branch	DC MCB	6 A
Inverter input	DC MCB	20 A
AC output	RCBO	3 A

F. System Architecture and Design

The complete system integrates energy generation, storage, power conditioning, electrical protection, and IoT-based monitoring within a single pole-mounted smart platform. The photovoltaic (PV) module is installed at the top of the pole to maximize solar irradiance exposure and minimize shading losses. Directly below the PV module, the LED luminaire and CCTV unit are mounted to ensure optimal illumination distribution and surveillance coverage, supporting both public safety and urban monitoring functions.

The $LiFePO_4$ battery pack is installed longitudinally inside a sealed IP-rated enclosure positioned within the pole structure to enhance mechanical stability, thermal management, and environmental protection against moisture, dust, and vandalism. This vertical blade-type arrangement improves structural rigidity while maintaining compact integration within limited pole dimensions. All power electronic components—including the MPPT charge controller, DC and AC protection devices, inverter, and communication modules—are housed in a lockable panel box located at an accessible height to ensure operational safety, simplified maintenance, and secure access control.

Energy flows hierarchically through a modular DC bus architecture, beginning with PV energy conversion via the MPPT controller, followed by battery storage regulation, and subsequently distributed to DC and AC loads. This structured topology allows independent branch protection, selective coordination, and simplified fault diagnosis. The integration of IoT-based wireless monitoring enables real-time observation of voltage, current, state of charge (SOC), temperature, and load status, facilitating predictive maintenance and remote system management.

The unified mechanical–electrical configuration enhances structural durability, operational resilience, and scalability. By consolidating all subsystems within a single smart pole platform, the design minimizes external wiring complexity, reduces installation footprint, and supports modular expansion for future smart city applications. An illustration of the overall system architecture is presented in Figure 2, while the detailed mechanical and physical design of the proposed installation is shown in Figure 3.

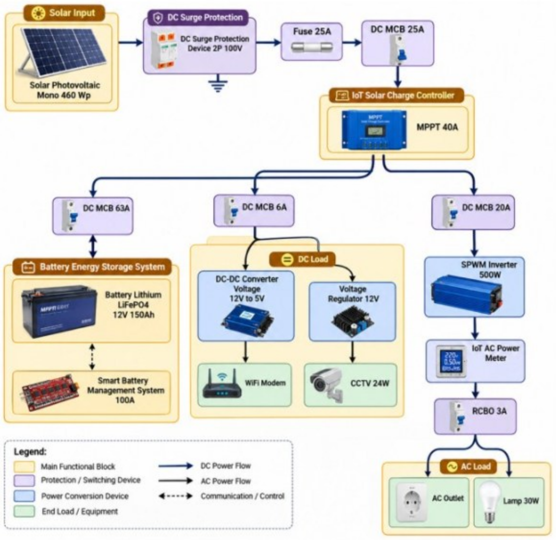

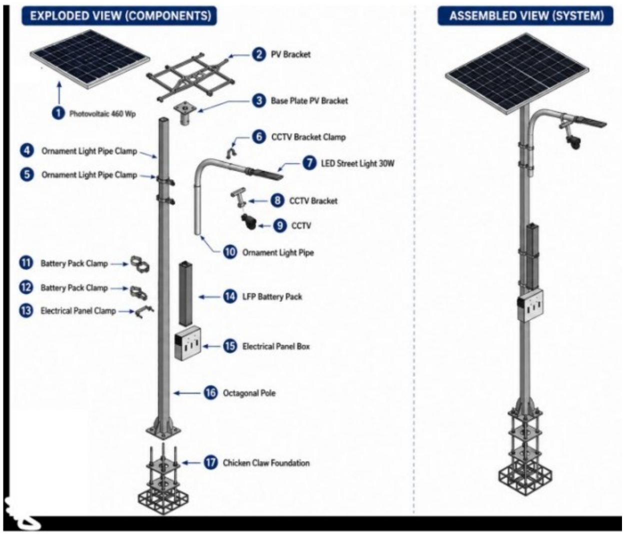

Figure 2. Proposed System Architecture **Figure 3. Proposed System Design**

III. Results and Discussion

A. Solar Irradiance Survey and Installation Site Selection

(a) (b) (c)

Figure 4. Solar Irradiance Survey and Installation Site Selection

An on-site solar irradiance survey was conducted to verify that the selected installation site could provide sufficient solar exposure to sustain the designed daily energy demand of 1529 Wh/day. Accurate characterization of local solar resources is essential for standalone photovoltaic (PV) systems because energy yield strongly depends on irradiance variability, shading conditions, and installation geometry, which directly influence charging reliability, battery recovery, and overall system autonomy [10], [30]. Field measurements were performed using a Lutron SPM-1116SD solar power meter, as illustrated in Figure 4(a), where the sensor was positioned in an open area free from surrounding obstructions to ensure representative global horizontal irradiance readings. Measurements were recorded at regular intervals over three consecutive clear-sky days in Keputih Village, Surabaya, covering morning, midday, and afternoon periods to capture the complete diurnal profile.

The measured results, as seen in Figure 4(b), peak solar intensity occurred between 11:30 and 13:30, reaching 890–1144 W/m², while morning and late-afternoon values declined to approximately 180–320 W/m² due to lower solar elevation angles. The calculated daily Global Horizontal Irradiance (GHI) averaged 5.1 kWh/m²/day, which exceeds the conservative design assumption of 4.5 Peak Sun Hours (PSH) used during system sizing. This additional irradiation margin increases the expected daily PV energy yield, enhances battery charging recovery, and reduces the risk of energy deficits during partially cloudy or transient weather conditions.

Based on these findings, the 460 Wp monocrystalline PV module was installed in an unobstructed location with northward orientation and a 10° tilt angle to maximize annual solar capture, consistent with Surabaya's latitude and local installation recommendations [39], [40]. The geographical placement of the system is shown in Figure 4(c), located near the intersection of Jl. Raya Marina Asri and Jl. Medokan Keputih. This site was selected not only for its high solar exposure and minimal shading losses but also for its functional urban advantages. The intersection provides an elevated and wide field of view for the integrated CCTV, enabling broader surveillance coverage of vehicular and pedestrian activities, particularly near Taman Harmoni public park. Consequently, the selected location simultaneously optimizes renewable energy harvesting and public safety monitoring. The irradiance survey confirms that the site offers sufficient and reliable solar resources to sustain autonomous system operation, while the strategic placement supports enhanced surveillance capability. These results validate both the technical feasibility and functional suitability of the proposed smart pole deployment within an urban smart city context.

B. Battery Pack Performance Testing

Experimental characterization of the 4S 150 Ah lithium iron phosphate ($LiFePO_4$) battery pack was conducted to validate the actual capacity, voltage stability, and the effectiveness of the integrated Battery Management System (BMS), since reliable storage performance is fundamental in standalone photovoltaic systems where available stored energy directly determines nighttime autonomy and overall system reliability. Testing was performed using a DK-Tester DSF40 under controlled charge–discharge cycling with continuous monitoring of voltage, current, and accumulated capacity. The experimental setup is presented in Figure 5(a), where the battery pack is connected to the programmable tester for regulated current injection and real-time data acquisition. Prior to testing, state-of-charge (SOC) calibration was executed by fully charging all cells and synchronizing the BMS to 100% to ensure that measured capacity accurately reflected the usable energy.

During charging, a constant current–constant voltage (CC–CV) profile of 20 A (0.133 C-rate) was applied until the terminal voltage reached 14.4 V, after which the current gradually tapered. The resulting charge curve shown in Figure 5(b) exhibits the characteristic $LiFePO_4$ voltage plateau, indicating stable electrochemical behavior and effective cell balancing across the series-connected pack. For discharge-capacity verification, a constant current of 40 A, equivalent to approximately 0.27C for the 150 Ah battery pack, was applied as an accelerated laboratory test as presented in Figure 5(c). This current was intentionally higher than the typical field-operating demand of approximately 5 A and was not intended to reproduce normal operating conditions. The objective was to reduce the test duration while evaluating the delivered capacity, voltage stability, and BMS cutoff behavior under a controlled and more demanding condition.

Because the available capacity and terminal-voltage response of lithium-ion batteries depend on the discharge rate [41], the measured capacity of 151 Ah is reported specifically at a discharge rate of 0.27C. The result should therefore not be interpreted as the exact capacity available under the lower field-operating current. Future work will include a low-rate discharge test that reproduces the actual lighting, CCTV, and modem load profile.

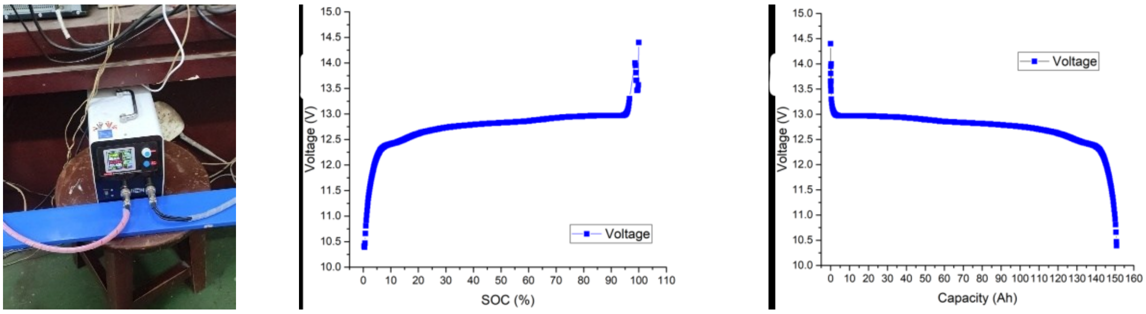

(a) (b) (c)

Figure 5. Battery Pack Performance Testing

C. Laboratory-Scale System Testing: MPPT Charging Performance

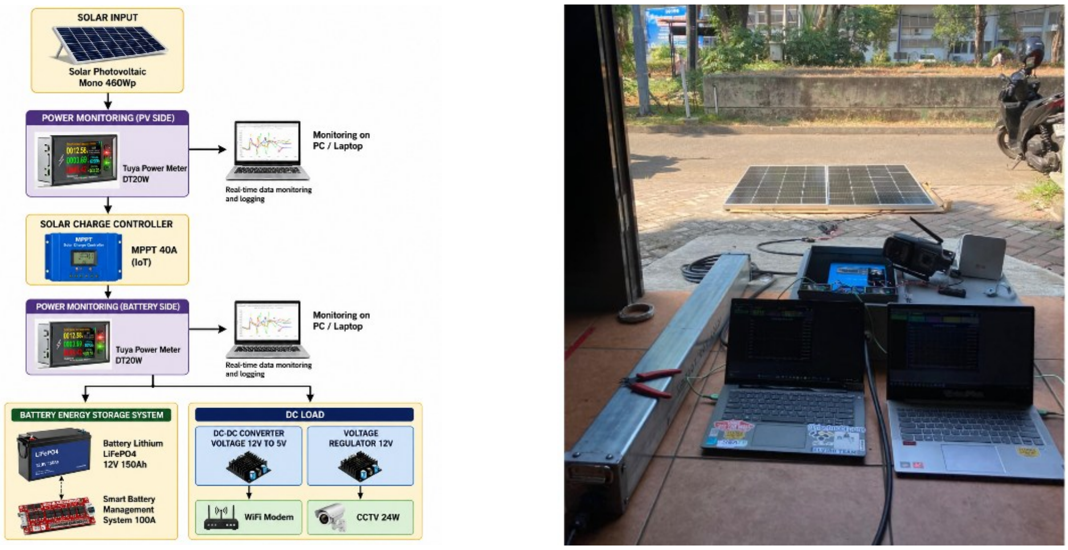

(a) (b)

Figure 6. Laboratory-Scale System Testing: MPPT Charging Performance Experimental Setup

Laboratory-scale testing was performed to validate the energy harvesting and charging performance of the PV–MPPT–battery subsystem. The setup consisted of a 460 Wp photovoltaic module, a 40 A MPPT controller, and a 150 Ah $LiFePO_4$ battery with representative DC loads. Electrical parameters were monitored using a digital power meter and data acquisition system. The measurements from 07:32 to 15:44 showed a typical daily PV generation pattern, with increasing morning output, a midday peak, and a gradual afternoon decrease. The PV system generated a total energy of 1309 Wh with a maximum power output of approximately 256 W, as shown in Figure 7(a).

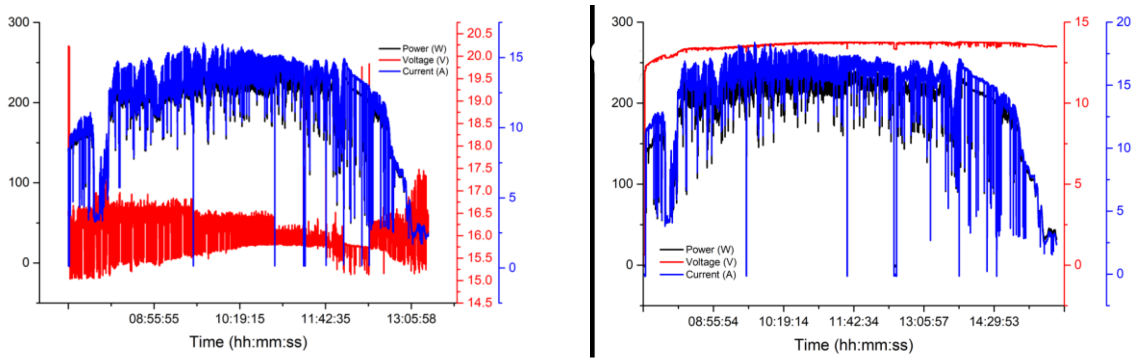

(a) (b)

Figure 7. PV and MPPT Charging Performance

Although the measured output was below the module's rated capacity of 460 Wp due to environmental factors such as irradiance variation, temperature effects, and system losses, the MPPT controller effectively optimized energy extraction. The normalized peak output ratio of 55.7% (256/460 W) indicates realistic field performance under non-ideal conditions. The MPPT charging profile demonstrated proper three-stage operation (bulk, boost, and float), ensuring efficient energy storage and voltage regulation. During testing, the battery SOC increased from 50% to 90% while supporting active loads, confirming that the PV–MPPT–battery subsystem provided sufficient energy generation and storage capability. These results validate the reliability and feasibility of the proposed standalone smart street lighting system for continuous operation of lighting, surveillance, and communication devices

D. Field Testing: Daily Energy Consumption, SoC, and DoD

Field testing over five consecutive days, from January 16 to January 20, 2026, was conducted to evaluate the real-world energy balance and short-term system autonomy. Across the five-day observation period, the post-charging SOC measured at 18:00 ranged from 90.0% to 97.2%, while the next-morning SOC ranged from 58.6% to 68.4%. The SOC-based nighttime energy consumption was estimated by multiplying the observed SOC reduction by the predefined usable battery-energy window of 1536 Wh, corresponding to an allowable depth of discharge of 80%. The average nighttime SOC reduction was 32.8%, corresponding to approximately 504 Wh/night. The recorded nighttime reductions ranged from 25.1% to 37.3%, equivalent to 386-573 Wh/night.

The LED luminaire consumed 300-320 Wh/night, with an average of 308 Wh/night. The difference between the SOC-based total night-time energy and the directly metered lighting energy ranged from 66 to 273 Wh/night, with an average of 196 Wh/night. The rated CCTV and modem power values were used as conservative inputs during system sizing. The lower field-measured night-time energy consumption compared with the nameplate-based estimate indicates that the actual operating power of these auxiliary loads may have been lower than their rated values. However, their individual energy consumption was not measured separately. This remaining energy was associated with the CCTV, communication modem, power-conversion losses, and uncertainty in SOC-based energy estimation. Therefore, lighting remained the largest single night-time load, although the auxiliary consumption was not negligible. During the monitored field period, daytime charging was sufficient to restore the battery SOC to 90.0–97.2%. This result indicates a positive short-term energy balance under the observed weather and load conditions. This operating profile may help limit excessive battery discharge and supported continuous service during the five-day observation period. The summarized results in Table 2 verify that the proposed 460 Wp PV and 150 Ah storage configuration reliably supports autonomous field operation.

Table 2. Daily SOC and Nighttime Energy Consumption During Five-Day Field Testing

Date	Weather	SoC 18:00 GMT+7 (%)	SoC 06:00 GMT+7 next day (%)	Night Drop (%)	Nighttime Energy (Wh)	Lighting Energy (Wh)
2026-01-16	Partly cloudy	90.0	58.6	31.4	482	300
2026-01-17	Sunny	96.4	59.1	37.3	573	300
2026-01-18	Sunny	97.2	60.0	37.2	571	320
2026-01-19	Sunny	96.9	63.8	33.1	508	320
2026-01-20	Light clouds	93.5	68.4	25.1	386	300
Average		**94.8**	**62.0**	**32.8**	**504**	**308**

Note:
Nighttime energy was estimated from the SOC reduction relative to the predefined usable battery-energy window of 1536 Wh

E. Functional and IoT System Performance Testing and Implications for Smart City Deployment

(a) (b) (c) (d)

Figure 8. Proposed System Implementation and Operation

Field implementation verified the successful integration of illumination, surveillance, and IoT-based monitoring within a single autonomous smart pole. Figure 8(a) presents the complete solar smart pole installed on-site, integrating a photovoltaic module, LED luminaire, CCTV camera, and communication devices into a compact standalone structure. The internal electrical configuration is depicted in Figure 8(b), which shows the organized arrangement of the $LiFePO_4$ battery pack, MPPT charge controller, inverter, protection components, and IoT modules. Nighttime functionality is confirmed in Figure 8(c), where the luminaire automatically operates according to the RTC schedule, while Figure 8(d) demonstrates the smartphone-based CCTV live-stream interface, validating remote accessibility and real-time surveillance capability. Collectively, these results confirm cohesive subsystem integration and reliable operation under real outdoor conditions.

Figure 9 illustrates the IoT monitoring framework that enables comprehensive supervision of system generation, storage, and consumption. Figure 9(a) shows the Battery Management System (BMS) interface reporting battery voltage, current, temperature, and state-of-charge (SOC) for continuous assessment of storage health. Figure 9(b) presents the MPPT dashboard displaying photovoltaic voltage, charging current, and instantaneous power to evaluate real-time harvesting efficiency. Figure 9(c) depicts AC-side energy measurements from the IoT power meter for the lighting subsystem, while Figure 9(d) summarizes daily accumulated energy records to support trend analysis and energy-balance evaluation. These unified dashboards facilitate remote diagnostics, preventive maintenance, and operational optimization.

Functional tests further demonstrated stable and synchronized performance. The RTC-based lighting controller achieved automatic switching, ensuring accurate scheduling. The CCTV subsystem operated continuously with stable 8 MP H.265X video streaming. The IoT communication system achieved an availability above 99% during the observation period, and no prolonged communication interruption or system shutdown was observed.

From a smart city perspective, the integrated architecture provides several practical benefits. The solar-powered configuration avoids grid-electricity purchases during autonomous operation, continuous surveillance enhances situational awareness, and centralized IoT monitoring supports remote diagnostics and data-driven infrastructure management. Overall, the system demonstrates short-term technical feasibility and energy autonomy under the observed conditions, indicating its potential for further development as sustainable smart city infrastructure.

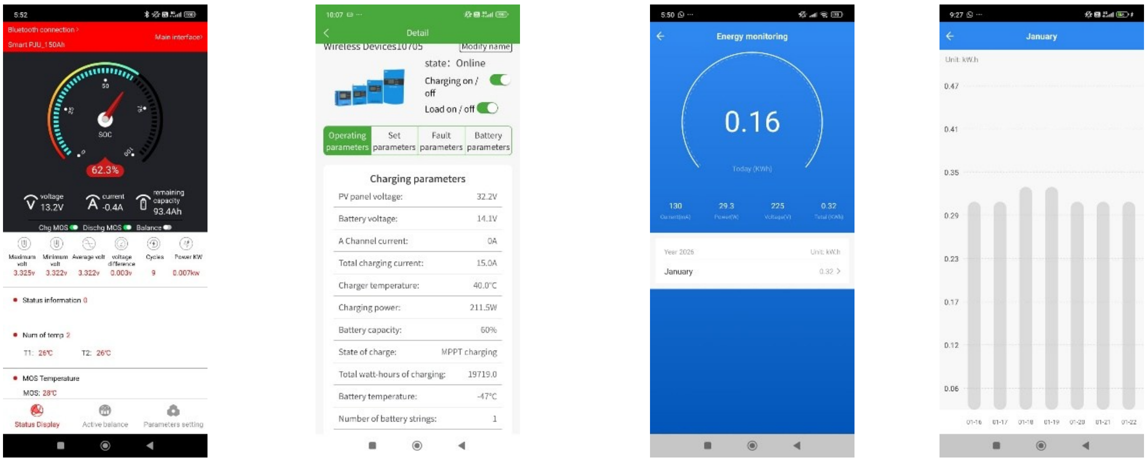

(a) (b) (c) (d)

Figure 9. The Performance of the IoT-Based Real-Time Monitoring System

F. Study Limitations and Future Validation

The field campaign was conducted for five consecutive days at a single urban location. Therefore, the results demonstrate short-term technical feasibility under the observed sunny, partly cloudy, and lightly cloudy conditions, but they do not establish year-round system reliability. The measurement period did not capture prolonged low-irradiance events, heavy wet-season rainfall, seasonal changes in solar geometry, extended shading, module soiling, battery aging, or site-to-site environmental variability.

Previous photovoltaic street-lighting studies have demonstrated that monthly solar-resource variation, storage-system characteristics, and local operating conditions can substantially influence energy production, reliability, and economic performance [5], [23], [42]. Future work will therefore extend field monitoring across dry and wet seasons and at multiple installation sites. The extended evaluation will include daily energy balance, loss-of-load probability, battery temperature and degradation, communication availability, module soiling, maintenance events, and component-replacement requirements.

G. Preliminary Economic Comparison

The designed system has an estimated daily energy demand of 1.176 kWh/day, corresponding to approximately 429.24 kWh/year. For an equivalent grid-powered system, the annual electricity cost can be estimated using (21).

$$C_{grid} = E_{annual} \, x \, T_{grid} \tag{21}$$

where E_{annual} is the annual electricity consumption and T_{grid} is the applicable electricity tariff. Using an illustrative public-street-lighting tariff of Rp1,699.53/kWh, the annual grid electricity expenditure is approximately Rp729,506 per pole. The P-3/TR tariff was reported at Rp1,699.53/kWh, while the Indonesian government maintained nonsubsidized tariff levels during subsequent tariff periods [43].

During autonomous operation, the proposed solar-powered system does not purchase electricity from the grid. However, it requires higher initial investment due to the photovoltaic module, battery, MPPT controller, inverter, protection devices, supporting structure, and installation. It also incurs future battery and power-electronics replacement costs. Therefore, the present results demonstrate reduced grid-electricity purchases rather than a confirmed reduction in total life-cycle cost. A complete economic evaluation should include capital expenditure, grid-connection or grid-extension cost, maintenance, battery replacement, discount rate, residual value, net present value, discounted payback period, and levelized cost of electricity (LCOE) [5], [23], [42]. A preliminary comparison with an equivalent grid-powered system is presented in Table 3.

Table 3. Preliminary Comparison Table

Parameter	Conventional Grid-Powered System	Proposed Solar-Powered System
Daily electrical demand	1.176 kWh/day	1.176 kWh/day
Annual electrical demand	429.24 kWh/year	429.24 kWh/year
Annual grid-energy purchase	429.24 kWh	Approximately 0 kWh
Illustrative annual electricity cost	Approximately Rp729,506	Approximately Rp0 for grid energy
Initial investment	Lower if an existing grid connection is available	Higher due to PV, battery, MPPT, and inverter
Main long-term expenditure	Electricity tariff and grid maintenance	Battery and power-electronics replacement
Main advantage	Lower initial cost in grid-served locations	Energy autonomy and avoided grid extension

Table 3 compares the conventional grid-powered system and the proposed solar-powered system in terms of energy demand, cost, and operational advantages. Both systems require the same annual energy consumption of 429.24 kWh/year, but the grid-based system depends entirely on purchased electricity, while the solar system can reduce grid energy consumption to nearly zero. Although the solar system requires higher initial investment for PV panels, batteries, MPPT, and inverter components, it provides long-term benefits through energy autonomy and reduced dependence on grid infrastructure

IV. CONCLUSION

This study designed, implemented, and experimentally evaluated a standalone solar-powered smart street lighting system integrating LED illumination, CCTV surveillance, and IoT-based monitoring within a single pole-mounted platform. Load analysis identified a demand of 1176 Wh/day and a design requirement of 1529 Wh/day after applying a 30% margin. Based on these requirements, a 460 Wp monocrystalline photovoltaic module, a 40 A MPPT charge controller, and a 12.8 V, 150 Ah $LiFePO_4$ battery were selected. The design calculations estimated 1863 Wh/day of usable photovoltaic energy and 1536 Wh of usable battery storage at an allowable depth of discharge of 80%. Accelerated battery testing at 0.27C measured a capacity of 151 Ah, while laboratory testing demonstrated the expected bulk/MPPT, boost, and float charging behavior.

During five consecutive days of field testing, the post-charging SOC ranged from 90.0% to 97.2%, the next-morning SOC remained between 58.6% and 68.4%, and the average nighttime SOC reduction was 32.8%. The IoT platform enabled real-time monitoring of photovoltaic generation, battery condition, and load operation, with communication availability exceeding 99% during the observation period. These findings demonstrate short-term autonomous operation and technical feasibility under the observed environmental and load conditions. The preliminary economic comparison indicates that the proposed system can avoid grid-electricity purchases during autonomous operation, but it does not establish lower total life-cycle costs. Long-term monitoring across dry and wet seasons, low-rate battery testing under the actual load profile, multi-site deployment, component-degradation assessment, and complete life-cycle cost analysis are required before year-round reliability and economic competitiveness can be concluded.

ACKNOWLEDGEMENT

The researchers express their sincere gratitude to the Politeknik Elektronika Negeri Surabaya (PENS), particularly the Research and Community Service Center (P3M), for the financial support provided through the Community Service Program Funding based on the Decree of the Director of Politeknik Elektronika Negeri Surabaya No. 98/PL14/PM/IV/2025 concerning the Funding for the Implementation of Community Service Activities at P3M PENS in 2025. The researchers also would like to extend their appreciation to the ELVIRO Team and the Industrial Electrical Engineering Study Program of PENS for their valuable contributions, assistance, and support during the implementation of this program.

REFERENCES

[1] P. Mohanty, U. C. Pati, K. Mahapatra, and S. P. Mohanty, "bSlight : Battery-Less Energy Autonomous Street Light Management System for Smart City," *IEEE Trans. Sustain. Comput.*, vol. 9, no. 1, pp. 100–114, 2024, https://doi.org/10.1109/TSUSC.2023.3310884.

[2] P. Tsankov, M. Yovchev, and H. Ibrishimov, "Energy-efficient light-emitting diode retrofit and advanced control in municipal street lighting : A case study from Bulgaria," *Asian J. Water, Environ. Pollut.*, vol. 22, no. 6, pp. 180–197, 2025, https://doi.org/10.36922/AJWEP025310242.

[3] A. Velu, R. Ramamoorthy, S. M. Manasa, and D. Navulkumar, "An Energy Efficient IoT based Smart Street Lighting using Low Cost SOC," in *2024 International Conference on Electronics, Computing, Communication and Control Technology (ICECCC)*, Bengaluru, India: IEEE, 2024, pp. 1–6. https://doi.org/10.1109/ICECCC61767.2024.10593834.

[4] R. Sikora and P. Markiewicz, "Evaluation of Maintenance and Modernization of Road Lighting Systems Using Energy Performance Indicators," *Energies*, vol. 18, no. 16, pp. 1–19, 2025, https://doi.org/10.3390/en18164328.

[5] A. Ngaopitakkul and S. Yoomak, "Investigating the feasibility of nano-grid infrastructure integration into street lighting systems based on energy production and economic evaluation," *Sci. Rep.*, vol. 14, no. 29833, pp. 1–20, 2024, https://doi.org/10.1038/s41598-024-80689-4.

[6] A. Mdallal, A. Yasin, M. Mahmoud, M. Ali, A. Hai, and A. Ghani, "A comprehensive review on solar photovoltaics : Navigating generational shifts , innovations , and sustainability," *Sustain. Horizons*, vol. 13, no. 100137, pp. 1–20, 2025, https://doi.org/10.1016/j.horiz.2025.100137.

[7] A. Shahsavari and M. Akbari, "Potential of solar energy in developing countries for reducing energy-related emissions," *Renew. Sustain. Energy Rev.*, vol. 90, pp. 275–291, 2018, https://doi.org/10.1016/j.rser.2018.03.065.

[8] M. Aldhi, H. Satria, M. Mungkin, I. Dayana, and R. Salam, "Prototype Design of Remote Smart Car 4WD Robot Car with Additional Power Photovoltaic Source Integrated Arduino," *Int. J. Eng. Technol. Nat. Sci.*, vol. 6, no. 1, pp. 11–16, 2024, https://doi.org/10.46923/ijets.v6i1.291.

[9] J. Bian and J. J. Yang, "Smart Street Lighting Powered by Renewable Energy :," *Sustainability*, vol. 17, no. 13, pp. 1–19, 2025, https://doi.org/10.3390/su17135874.

[10] R. I. Putri, D. Radianto, Z. Amalia, A. G. Abdullah, D. Zakaria, and D. L. Hakim, "Development of a Real-Time Monitoring Model for Solar-Powered Street Lighting Systems Using Internet of Things," *Eng. Technol. Appl. Sci. Res.*, vol. 15, no. 6, pp. 29186–29193, 2025, https://doi.org/10.48084/etasr.13063.

[11] M. A. Rahman, M. Y. Mukta, A. Yousuf, A. T. Asyhari, Z. A. Bhuiyan, and C. Y. Yaakub, "IoT based Hybrid Green Energy Driven Highway Lighting System," in *2019 IEEE Intl Conf on Dependable, Autonomic and Secure Computing, Intl Conf on Pervasive Intelligence and Computing, Intl Conf on Cloud and Big Data Computing, Intl Conf on Cyber Science and Technology Congress (DASC/PiCom/CBDCom/CyberSciTech)*, Fukuoka, Japan: IEEE, 2019, pp. 587–594. https://doi.org/10.1109/DASC/PiCom/CBDCom/CyberSciTech.2019.00114.

[12] D. Güneş, A. A. Şeker, and B. E. Türkay, "Off-Grid Surveillance Powered by Solar Energy : A Comparative Study of MPPT Algorithms," *Energies*, vol. 19, no. 2, pp. 1–29, 2026, https://doi.org/10.3390/en19020489.

[13] A. Ngaopitakkul, P. Songsukthawan, S. Bunjongjit, B. Sreewirote, S. Yoomak, and C. Pothisarn, "Design and techno-economic evaluation of a nanogrid system for a small-scale public railway station building in Thailand," *Results Eng. J.*, vol. 28, no. 107648, pp. 1–21, 2025, https://doi.org/10.1016/j.rineng.2025.107648.

[14] J. Li, M. He, P. C.-I. Pang, and C.-T. Lam, "An Easy-to-install Rear-Mountable Intelligent Street Light with Companion App for Mitigations of Urban Traffic Problems," in *2022 6th International Conference on Universal Village (UV)*, Boston, MA, USA: IEEE, 2022, pp. 1–8. https://doi.org/10.1109/UV56588.2022.10185509.

[15] S. J. Anjani, B. Kusbandrijo, and S. Hartono, "Implementasi Program Surabaya Integrated Command Center (SICC) Sebagai Upaya Peningkatan Smart City Di Surabaya," *PRAJA Obs. J. Penelit. Adm. Publik*, vol. 4, no. 03, pp. 193–204, 2024. https://aksiologi.org/index.php/praja/article/view/1536

[16] A. Arisman and I. Iwan, "Effectiveness of Solar Panel-Based Street Lights and Their Impact on Environmental Sustainability," *Res. Horiz.*, vol. 3, no. 6, pp. 646–654, 2023, https://doi.org/10.54518/rh.3.6.2023.189.

[17] M. A. Akbar and T. N. Azhar, "Concept of Cost Efficient Smart CCTV Network for Cities in Developing Country," in *2018 International Conference on ICT for Smart Society (ICISS)*, Semarang, Indonesia: IEEE, 2018, pp. 1–4. https://doi.org/10.1109/ICTSS.2018.8550016.

[18] R. Raman, K. R. Naikade, M. P. Aarthi, S. Sujatha, and D. Vekariya, "Cloud-Based Solar Lights for Sustainable Cities : Real-time Monitoring and Energy Efficiency Solutions," in *2023 Second International Conference On Smart Technologies For Smart Nation (SmartTechCon)*, IEEE, 2023, pp. 1288–1292. https://doi.org/10.1109/SmartTechCon57526.2023.10391346.

[19] P. Mohanty, U. C. Pati, and K. Mahapatra, "Self-Powered Intelligent Street Light Management System for Smart City," in *2021 IEEE 18th India Council International Conference (INDICON)*, Guwahati, India: IEEE, 2021, pp. 1–6. https://doi.org/10.1109/INDICON52576.2021.9691575.

[20] T. F. Vieira, D. B. Brito, M. Ribeiro, and Í. Araújo, "An IoT Based Smart Utility Pole and Street Lighting System," in *2019 IEEE CHILEAN Conference on Electrical, Electronics Engineering, Information and Communication Technologies (CHILECON)*, Valparaiso, Chile, 2019, pp. 1–5. https://doi.org/10.1109/CHILECON47746.2019.8987690.

[21] A. Quattrocchi, F. Martella, V. Lukaj, R. De Leo, M. Villari, and R. Montanini, "Designing a Low-Cost System to Monitor the Structural Behavior of Street Lighting Poles in Smart Cities," *Sensors*, vol. 23, no. 15, pp. 1–16, 2023, https://doi.org/10.3390/s23156993.

[22] S. Vadi, "Design and Implementation of an Off-Grid Smart Street Lighting System Using LoRaWAN and Hybrid Renewable Energy for Energy-Efficient Urban Infrastructure," *Sensors*, vol. 25, no. 17, pp. 1–33, 2025, https://doi.org/10.3390/s25175579.

[23] P. Chiradeja, S. Yoomak, and A. Ngaopitakkul, "Economic Analysis of Improving the Energy Efficiency of Nanogrid Solar Road Lighting Using Adaptive Lighting Control," *IEEE Access*, vol. 8, pp. 202623–202638, 2020, https://doi.org/10.1109/ACCESS.2020.3035702.

[24] L. Baumgärtner, J. Höchst, P. Lampe, R. Mogk, A. Sterz, and P. Weisenburger, "Smart Street Lights and Mobile Citizen Apps for Resilient Communication in a Digital City," in *2019 IEEE Global Humanitarian Technology Conference (GHTC)*, Seattle, WA, USA, 2019, pp. 1–8. https://doi.org/10.1109/GHTC46095.2019.9033134.

[25] O. Petrosian and Y. Zhang, "Solar Power Generation Forecasting in Smart Cities and Explanation Based on Explainable AI," *Smart Cities*, vol. 7, no. 6, pp. 3388–3411, 2024, https://doi.org/10.3390/smartcities7060132.

[26] H. Louie and P. Dauenhauer, "Effects of load estimation error on small-scale off-grid photovoltaic system design , cost and reliability," *Energy Sustain. Dev.*, vol. 34, pp. 30–43, 2016, https://doi.org/10.1016/j.esd.2016.08.002.

[27] Y. G. Cusa, J. H. Suárez, J. L. M. Rodríguez, T. H. Ramírez, S. A. B. V. De Melo, and E. A. Torres, "Optimal Sizing of an Off-Grid Hybrid Energy System with Metaheuristics and Meteorological Forecasting Based on Wavelet Transform and Long Short-Term Memory Networks," *Energies*, vol. 18, no. 20, pp. 1–34, 2026, https://doi.org/10.3390/en18205371.

[28] E. Chang, R. Wu, H. H. Chang, and C. Cheng, "Study and Implementation of a High-Quality True Sine Wave DC-to-AC Inverter for Solar Power Generation Systems," *Micromachines*, vol. 13, no. 10, pp. 1–17, 2022, https://doi.org/10.3390/mi13101723.

[29] A. Zeghoudi, A. Bendaoud, L. Canale, A. Tilmatine, and H. Slimani, "Determination of Power Factor and Harmonic Distortion of AC / DC LED Driver," in *2021 IEEE International Conference on Environment and Electrical Engineering and 2021 IEEE Industrial and Commercial Power Systems Europe (EEEIC / I&CPS Europe)*, Bari, Italy: IEEE, 2021, pp. 1–6. https://doi.org/10.1109/EEEIC/ICPSEurope51590.2021.9584665.

[30] P. Megantoro, M. A. Syahbani, I. H. Sukmawan, S. D. Perkasa, and P. Vigneshwaran, "Effect of peak sun hour on energy productivity of solar photovoltaic power system," *Bull. Electr. Eng. Informatics*, vol. 11, no. 5, pp. 2442–2449, 2022, https://doi.org/10.11591/eei.v11i5.3962.

[31] A. Al Mansur, M. R. Amin, and K. K. Islam, "Performance Comparison of Mismatch Power Loss Minimization Techniques in Series-Parallel PV Array Configurations," *Energies*, vol. 12, no. 5, pp. 1–21, 2019, https://doi.org/10.3390/en12050874.

[32] R. M. Smith, M. Matam, and H. Seigneur, "Mismatch losses in a PV system due to shortened strings," *Energy Convers. Manag.*, vol. 250, no. 114891, 2021, https://doi.org/10.1016/j.enconman.2021.114891.

[33] E. N. Sholikhah, A. R. Annisa, M. R. Rusli, and M. Putri, "A Simple Modeling of MPPT-based ANN for Photovoltaic System," *J. Comput. Electron. Telecommun.*, vol. 6, no. 1, pp. 1–9, 2025, https://doi.org/10.52435/complete.v6i1.684.

[34] T. Abuzairi, W. W. A. Ramadhan, and K. Devara, "Solar Charge Controller with Maximum Power Point Tracking for Low-Power Solar Applications," *Int. J. Photoenergy*, vol. 2019, pp. 1–11, 2019, https://doi.org/10.1155/2019/5026464.

[35] E. Faizal, Y. A. Winoko, M. S. Mustapa, and M. Kozin, "Solar Charger Controller Efficiency Analysis of Type Pulse Width Modulation (PWM) and Maximum Power Point Tracking (MPPT)," *Asian J. Sci. Eng.*, vol. 1, no. 2, 2022, https://doi.org/10.51278/ajse.v1i2.546.

[36] M. A. Hannan *et al.*, "Battery energy-storage system : A review of technologies , optimization objectives , constraints , approaches , and outstanding issues," *J. Energy Storage*, vol. 42, 2021, https://doi.org/10.1016/j.est.2021.103023.

[37] R. Dufo-López, T. Cortés-Arcos, J. S. Artal-Sevil, and J. L. Bernal-Agustín, "Comparison of Lead-Acid and Li-Ion Batteries Lifetime Prediction Models in Stand-Alone Photovoltaic Systems," *Appl. Sci.*, vol. 11, no. 3, 2021, https://doi.org/10.3390/app11031099.

[38] J. Gorsch *et al.*, "Contrasting a BYD Blade prismatic cell and Tesla 4680 cylindrical cell with a teardown analysis of design and performance," *Cell Reports Phys. Sci.*, vol. 6, no. 3, 2025, https://doi.org/10.1016/j.xcrp.2025.102453.

[39] W. S. Ebhota and P. Y. Tabakov, "Impact of Photovoltaic Panel Orientation and Elevation Operating Temperature on Solar Photovoltaic System Performance," *Int. J. Renew. Energy Dev.*, vol. 11, no. 2, pp. 591–599, 2022, https://doi.org/10.14710/ijred.2022.43676.

[40] K. Perhubungan, *Peraturan Menteri Perhubungan Nomor 27 Tahun 2018 tentang Alat Penerangan Jalan*. 2018. https://peraturan.bpk.go.id/Details/104286/permenhub-no-27-tahun-2018

[41] C. Armenta-deu, J. P. Carriquiry, and S. Guzmán, "Capacity correction factor for Li-ion batteries : Influence of the discharge rate," *J. Energy Storage*, vol. 25, no. July, 2019, https://doi.org/10.1016/j.est.2019.100839.

[42] A. C. Duman and Ö. Güler, "Techno-economic analysis of off-grid photovoltaic LED road lighting systems : A case study for northern, central, and southern regions of Turkey," *Build. Environ.*, vol. 156, no. April, pp. 89–98, 2019, https://doi.org/10.1016/j.buildenv.2019.04.005.

[43] G. Buana, "Tarif Listrik PLN per kWh 2025: Daftar Lengkap 13 Golongan Pelanggan," Media Indonesia. Accessed: Jul. 01, 2026. [Online]. Available: https://mediaindonesia.com/ekonomi/803091/tarif-listrik-pln-per-kwh-2025-daftar-lengkap-13-golongan-pelanggan